AD-A111 687 AEROSPACE CORP EL SEGUNDO CA F/G 10/3
IMPEDANCE OF AEROSPACE NICD CELLS UNDER OPEN CIRCUIT CONDITIONS--ETC(U)
JAN 82 A H ZIMMERMAN F04701-81-C-0082
UNCLASSIFIED TR-0082(2945-01)-1 SD-TR-81-109 NL

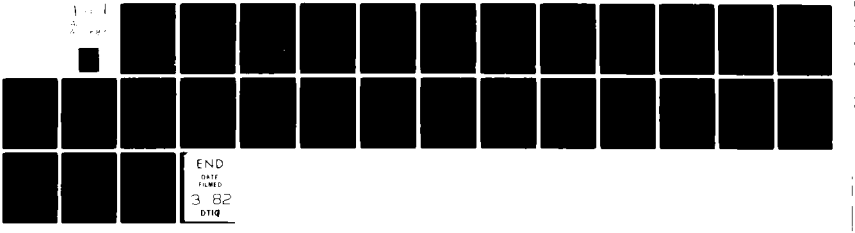

END
DATE FILMED
3 82
DTIC

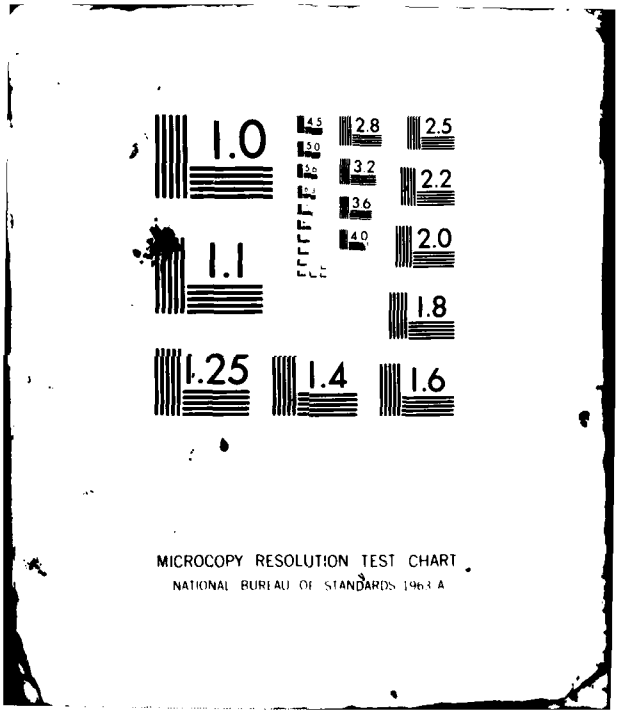
1.0
1.1
1.25
1.4
1.6
1.8
2.0
2.2
2.5
2.8
3.2
3.6
4.0
4.5
5.0
MICROCOPY RESOLUTION TEST CHART
NATIONAL BUREAU OF STANDARDS 1963 A

Impedance of Aerospace NiCd Cells Under Open Circuit Conditions

A. H. ZIMMERMAN
Laboratory Operations
The Aerospace Corporation
El Segundo, Calif. 90245

25 January 1982

Prepared for

AIR FORCE SPACE DIVISION
AIR FORCE SYSTEMS COMMAND
Los Angeles Air Force Station
P.O. Box 92960, Worldway Postal Center
Los Angeles, Calif. 90009

This interim report was submitted by The Aerospace Corporation, El Segundo, CA 90245, under Contract No. F04701-81-C-0082 with the Space Division, Deputy for Technology, P.O. Box 92960, Worldway Postal Center, Los Angeles, CA 90009. It was reviewed and approved for The Aerospace Corporation by S. Feuerstein, Director, Chemistry and Physics Laboratory. Lt Efren V. Fornoles, SD/YLXT, was the Project Officer for the Mission-Oriented Investigation and Experimentation (MOIE) Program.

This report has been reviewed by the Public Affairs Office (PAS) and is releasable to the National Technical Information Service (NTIS). At NTIS, it will be available to the general public, including foreign nations.

This technical report has been reviewed and is approved for publication. Publication of this report does not constitute Air Force approval of the report's findings or conclusions. It is published only for the exchange and stimulation of ideas.

Efren V. Fornoles

Efren V. Fornoles, 1st Lt, USAF
Project Officer

Florian P. Meinhardt

Florian P. Meinhardt, Lt Col, USAF
Director of Advanced Space Development

FOR THE COMMANDER

Norman W. Lee

Norman W. Lee, Jr., Colonel, USAF
Deputy for Technology

UNCLASSIFIED
SECURITY CLASSIFICATION OF THIS PAGE (When Data Entered)

REPORT DOCUMENTATION PAGE		READ INSTRUCTIONS BEFORE COMPLETING FORM
1. REPORT NUMBER SD-TR-81-109	2. GOVT ACCESSION NO. AD-A111687	3. RECIPIENT'S CATALOG NUMBER
4. TITLE (and Subtitle) IMPEDANCE OF AEROSPACE NiCd CELLS UNDER OPEN CIRCUIT CONDITIONS		5. TYPE OF REPORT & PERIOD COVERED 6. PERFORMING ORG. REPORT NUMBER TR-0082(2945-01)-1
7. AUTHOR(s) A. H. Zimmerman		8. CONTRACT OR GRANT NUMBER(s) F04701-81-C-0082
9. PERFORMING ORGANIZATION NAME AND ADDRESS The Aerospace Corporation El Segundo, Calif. 90245		10. PROGRAM ELEMENT, PROJECT, TASK AREA & WORK UNIT NUMBERS
11. CONTROLLING OFFICE NAME AND ADDRESS Space Division Air Force Systems Command Los Angeles, Calif. 90009		12. REPORT DATE 25 January 1982 13. NUMBER OF PAGES 24
14. MONITORING AGENCY NAME & ADDRESS(if different from Controlling Office)		15. SECURITY CLASS. (of this report) Unclassified 15a. DECLASSIFICATION/DOWNGRADING SCHEDULE

16. DISTRIBUTION STATEMENT (of this Report)

Approved for public release; distribution unlimited.

17. DISTRIBUTION STATEMENT (of the abstract entered in Block 20, if different from Report)

18. SUPPLEMENTARY NOTES

19. KEY WORDS (Continue on reverse side if necessary and identify by block number)

Nickel cadmium cell
Capacitance
Impedance
Diffusion
Alkaline electrolyte

20. ABSTRACT (Continue on reverse side if necessary and identify by block number)

The open circuit impedance of 10-A h sealed NiCd cells has been measured from 0 to 10^{-3} Hz as a function of cell state of charge and temperature. The open-circuit impedance at frequencies below 0.01 Hz is modeled by two consecutive diffusion-controlled charge transfer processes in the NiCd cell. Data analysis indicates that both solid-state diffusion processes and electrolyte diffusion processes are consistent with the data. Because concentration polarization is known to occur in NiCd cells, the two observed processes are tentatively

DD FORM 1473 (FACSIMILE)

UNCLASSIFIED
SECURITY CLASSIFICATION OF THIS PAGE (When Data Entered)

19. KEY WORDS (Continued)

20. ABSTRACT (Continued)

assigned to electrolyte diffusion in the positive and negative plates. The resolution of these processes in the impedance spectrum is sensitive to the relative pore structure and morphology of the electrode plates.

CONTENTS

FIGURES

IMPEDANCE OF AEROSPACE NiCd CELLS UNDER OPEN CIRCUIT CONDITIONS

I. INTRODUCTION

The impedance properties of battery cells provide a useful means for characterizing the processes that occur in a battery cell during both operating and open circuit conditions. For NiCd cells, impedance has been measured mainly in the audio frequency range. The work of Brodd and DeWane[1] demonstrated a notable inductive component in the impedance of sealed NiCd cells above several kilohertz, which was attributed to the physical structure of the cells. Gulton Industries[2] report the ac impedance of 20-A h cells in the frequency range 1 Hz to 100 kHz, as part of their effort to devise a state-of-charge indicator for NiCd batteries. In addition, there is a large body of literature[3-6] on NiCd cell impedances as a function of capacity at a fixed frequency, typically 1000 Hz. These results indicate that the impedance decreases as cell capacity increases;[6] this effect is likely to arise from decreased ohmic resistance as well as greater capacitance as cell capacity is increased. None of this work provides much detailed information on the chemical and physical processes of significance in NiCd cells. In fact, essentially no data exist on the impedance of NiCd cells at frequencies below 1 Hz, which is the range expected to be most important for diffusion processes and film growth.

Diffusion processes both in the alkaline electrolyte and in solid-state films at the electrodes are generally believed to be extremely important to the proper functioning of the NiCd cell. Diffusion of both OH^- and H_2O in the electrolyte must occur because these reagents are produced and consumed during cell charge and discharge. Work on planar Cd electrodes by Armstrong and Edmondson[7] has indicated that diffusion through a surface film is important in the passivation of the Cd electrode. An important step in the oxidation of the Ni electrode is believed to involve proton diffusion from the oxidation site to the electrode-electrolyte interface.[8] Diffusion coefficients and

activation energies for this process have been measured.[9] However, the problem of detecting and measuring these processes in the actual battery cell remains.

In this report, we present detailed measurements of the impedance of a 10-A h NiCd cell over frequencies ranging from 0 to 100 kHz. The impedance measurements at the low frequencies are expected to provide information on the electrolyte and solid-state diffusion processes that are important in the NiCd cell. The measurements also will add to the data base that is used for the application of NiCd cells. These cells are an important component of many secondary power systems in satellites, and, therefore, their impedance is a parameter that should be considered over as wide a frequency range as possible in the planning and operation of the power system.

II. EXPERIMENTAL

All experimental measurements were made with a 10-A h sealed NiCd cell. This cell was an aerospace quality cell (S/N L1-137) of prismatic design, manufactured by General Electric Company.* Before it was used and during storage periods longer than 4 days, the cell was stored in the shorted state. Preceding each experiment, the cell was brought to full charge by a 16-h charge at 1 A, then discharged to 1 V at 2.50 A, and finally recharged again for 16 h at 1 A. The cell capacity for the 2.50-A discharge rate was 12.7 A h. A Kepco KS36-15M power supply was used for cell charge and discharge.

Previous work[10] has indicated that NiCd cells have temperature coefficients of several hundred microvolts/°C. Therefore, it was necessary to precisely control the cell temperature during the galvanostatic transient measurements. The temperature of the cell was held constant to ±0.05°C per day in a thermally insulated compartment, which was immersed in a regulated temperature bath (Forma Scientific 2095). The differential amplifier and reference cell were contained in the same thermally regulated compartment as the cell, so thermal noise effects could be minimized. With this arrangement, thermal drift was limited to 10 to 20 μV per day and less than 1 μV per minute.

The galvanostatic transient technique was used to measure the impedance at frequencies below 1 Hz. The apparatus for these measurements consisted of a 1-mA constant current source, which was applied to the open circuit battery cell. A low-noise differential amplifier that has an input impedance of 10^{12} Ω was constructed in our laboratory to permit the change in cell voltage relative to a mercury cell to be monitored as a function of time. The voltage transient was monitored by the use of a strip chart recorder with a full scale pen response time of about 0.5 sec (Linear Instruments Model 141). Beginning

*G.E. Catalog No. 42B010AB08-G3.

with the cell near full charge, several transients were measured for 1 mA charge and discharge current steps. Then the cell was discharged at 2.5 A to a new state of charge and the measurements repeated until the cell was totally discharged. The cell had to stand at least 8 h between measurements to reattain the open circuit steady-state voltage. Because these experiments were spread over many days, the state of charge of the cell for each experiment had to be corrected for self-discharge. The self-discharge rate was found by noting the capacity difference between the freshly charged cell and the cell 30 days after charge. This self-discharge rate amounted to 0.75 to 1% per day.

Because of the relatively small voltage changes that were monitored (1 to 5 mV typical), the presence of noise would lead to severe problems. We found that after a 16-h charge at 1 A, the NiCd cell produced a noise signal that had a peak-to-peak amplitude of about 80 μV. This cell noise was in a very low frequency range, with periods from several minutes to an hour. The noise prevented experiments from being made with a newly charged cell. After 1 week of open circuit stand, the noise decreased to about 20 μV. Then after 1 A h of capacity was discharged, the noise further decreased to about 10 μV , which was an acceptable level for the experimental measurements. The background noise from the amplifier electronics was equivalent to 3 to 4 μV at frequencies less than 10 Hz. The source of the low-frequency cell-generated noise has not yet been established, although it was absent for a flooded NiCd cell.

Impedance was measured in the 10 Hz to 100 kHz frequency range by monitoring the in-phase and out-of-phase components of the voltage produced by an alternating current. The apparatus used for these measurements was based on a HP-3575A gain phase meter. The detailed configuration of this apparatus is described in Ref. 11.

III. RESULTS

Results of impedance measurements in the 10 Hz to 100 kHz range are indicated in Fig. 1. The impedance is quite low--several milliohms or less throughout this frequency range. The impedance exhibits small changes with state of charge at frequencies below 100 Hz, and generally becomes more resistive and more capacitive as the cell is discharged. In agreement with other work,[12-14] we found the impedance became inductive at frequencies higher than several hundred hertz. This effect is likely to result from the self inductance of the conductors in the cell as well as from distributed inductance caused by the porous structure of the electrodes.[15] The fact that the high-frequency inductive impedance of the cell is practically unaffected by the electrochemical state of the cell supports the theory that this inductance arises from the cell structure itself.

The impedance at very low frequencies (<1 Hz) was obtained from the transient voltage response of the cell to a 1-mA current step. The impedance was determined by assuming that the cell, when discharging, possessed a natural voltage change caused by the change in its state of charge, and that this natural behavior was linear in time. This assumption is expected to be valid when the transient is small enough that it does not noticeably perturb the electrochemical state of the cell. Transients less than roughly 5 mV appear to satisfy this criterion. The transient is monitored experimentally until the voltage becomes linear in time. The linear region gives the natural response, which is extrapolated back to zero time and subtracted from the data. The remaining transient response was converted to the frequency domain through a Laplace transformation. The current step was also transformed to the frequency domain, whereupon the ratio of voltage to current was used to obtain the impedance as a function of frequency.

Details of the conversion of a battery voltage transient to its impedance in the frequency domain are described in Ref. 11. Impedance data from a typical experiment are presented in Fig. 2 in the complex plane. In Fig. 3 the resistive and reactive components of the impedance are plotted as a function of $\omega^{-1/2}$.

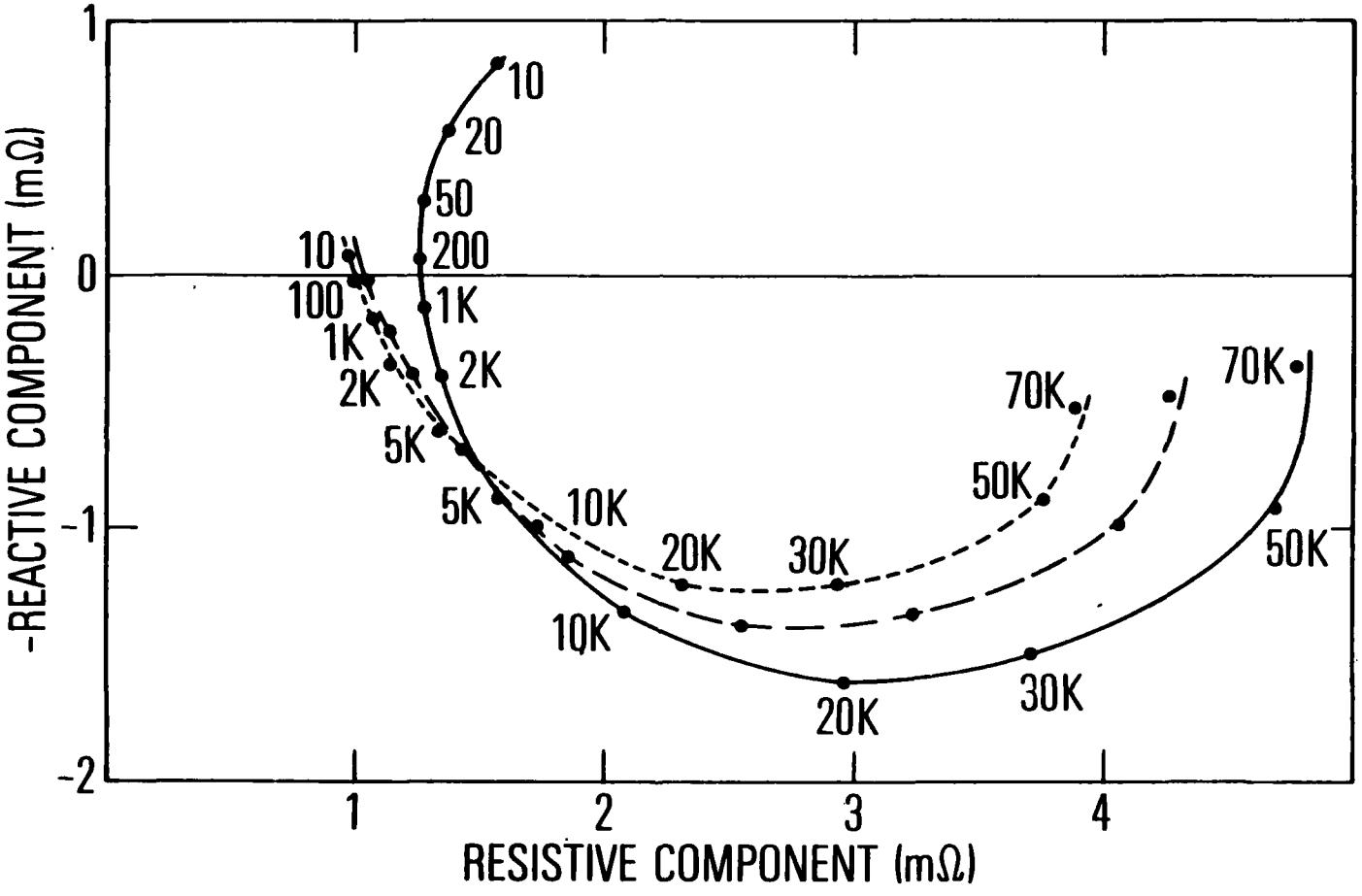

Fig. 1. Impedance of a 10-A h sealed NiCd cell in the Complex Plane at Full Charge (short dash), 44% of Full Charge (long dash), and Total Discharge (solid line). The numbers near the data points indicate frequency in Hz.

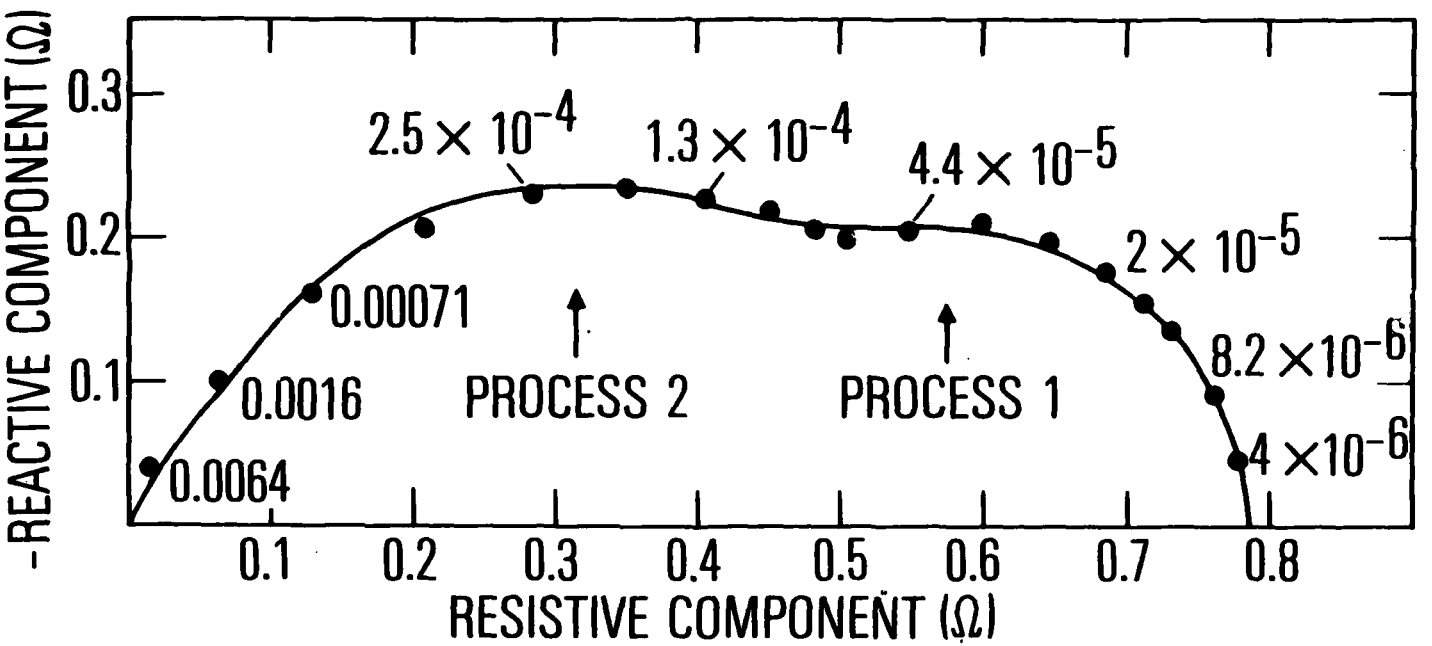

Fig. 2. Low Frequency Impedance of a 20% Charged 10-A h Sealed NiCd cell in the Complex Plane. The impedance measurement was made using a 1 mA discharging current step. The frequencies in Hz are noted next to each data point, and the solid line is a computer fit to the data. Temperature is 25°C.

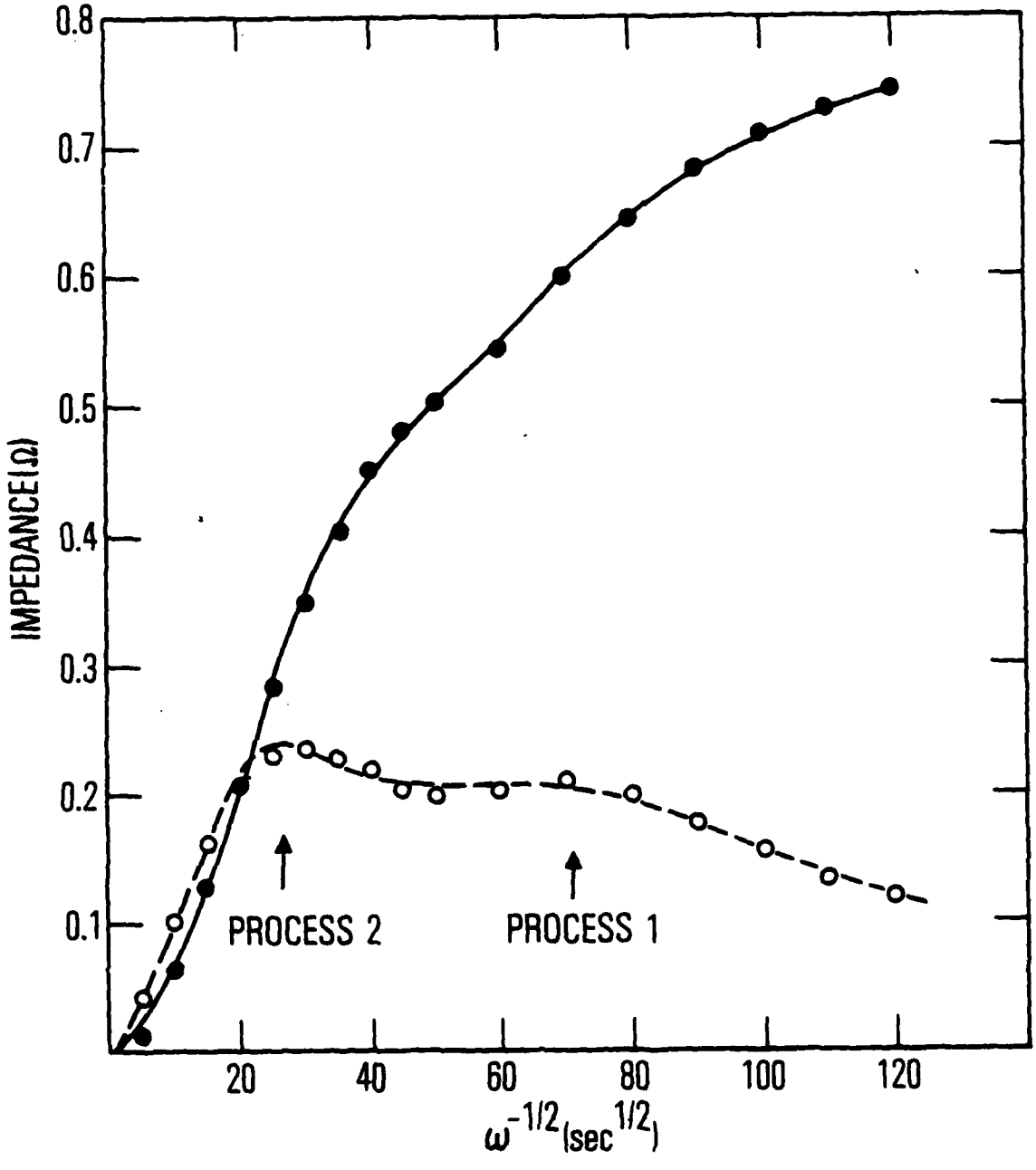

Fig. 3. Resistive (solid line) and Reactive (dashed line) Components of Impedance as a Function of $\omega^{-1/2}$. The experimental data are the same as for Fig. 2, and the lines represent the computer fit to the data using Eq. (8).

IV. DISCUSSION

The charge-discharge reactions at the electrodes in the NiCd cell involve transport of H_2O and OH^- ions through the cell as well as mass and charge transfer at the electrode-electrolyte interface. The overall electrode reactions can approximately be written as

$$NiOOH + H_2O + e^- \underset{\text{charge}}{\overset{\text{discharge}}{\rightleftharpoons}} OH^- + Ni(OH)_2 \qquad (1)$$

$$Cd + 2OH^- \underset{\text{charge}}{\overset{\text{discharge}}{\rightleftharpoons}} 2e^- + Cd(OH)_2 \qquad (2)$$

These reactions indicate that at low frequencies the impedance may be controlled by diffusive transport of OH^- and H_2O to and from the electrodes. Transport of these species may also be affected by the presence of films on the electrode surfaces. Diffusion transport will be coupled with the double-layer capacitance and charge-transfer resistance at each electrode in a manner that can be schematically represented by a Randles type circuit,[16] as indicated in Fig. 4. The double-layer capacitance is represented by C_{DL}. Capacitance that arises from surface species, or "pseudocapacitance," is represented by C_s, resistance to charge transfer at the electrode interface by R_{ct}, and the diffusion impedance or faradaic impedance by Z_D. Figure 4 also indicates a typical plot of the impedance in the complex plane when a single diffusion process controls the impedance. The linear portion, which rises from the origin at a 45-deg angle, results from semi-infinite diffusion control. In this linear regime, the diffusion gradients are not significantly affected by convective dissipation or boundary conditions during the period that corresponds to the frequencies in this regime. The effects of convection or boundaries eventually result in the diffusion layer approaching a steady-state condition. The steady-state condition is represented in Fig. 4 by the

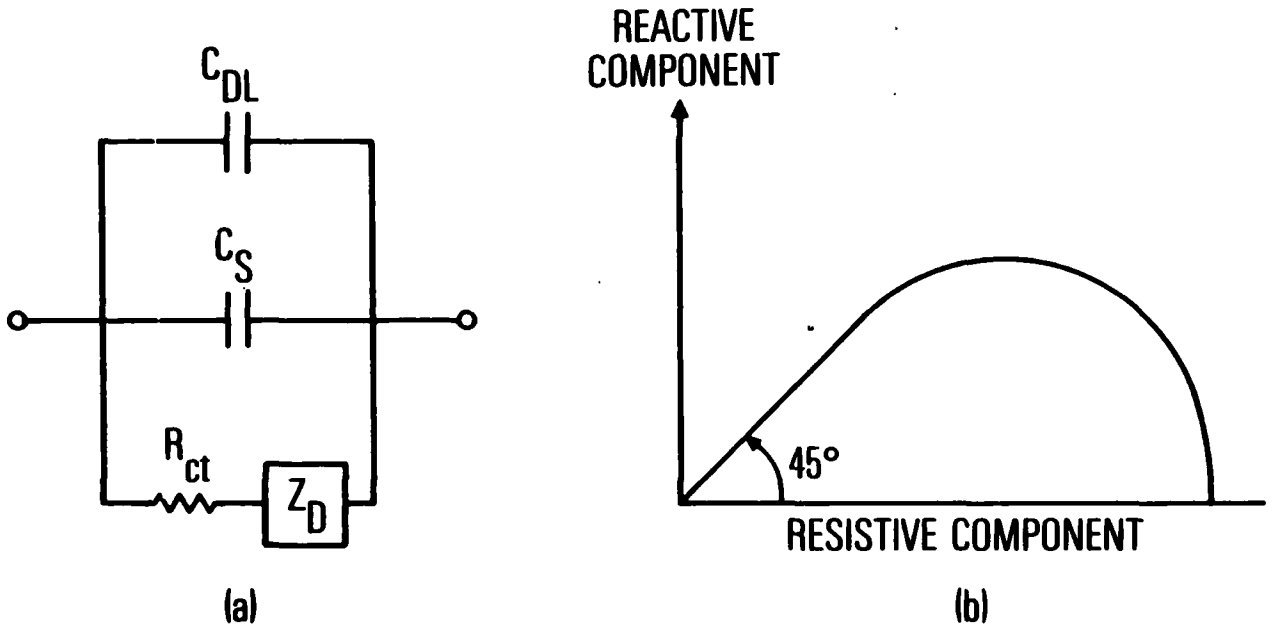

Fig. 4. (a) Equivalent Circuit for Electrode Process with Diffusion.

(b) Complex Plane Impedance for Equivalent Circuit with a Single Diffusion Process.

diffusion resistance R_o, and the approach to it by the semi-circular arc traced out in the complex plane as the frequency decreases.

A more quantitative description of the impedance from the equivalent circuit in Fig. 4 is obtained with the use of the analytical form for Z_D, which is a Warburg impedance.[17]

$$Z_D = \sigma\omega^{-1/2}(1 - j)\ \tanh\left(j^{1/2}\delta\sqrt{\frac{\omega}{D_o}}\right) \tag{3}$$

where σ is the Warburg coefficient, δ the diffusion layer thickness, D_o the diffusion coefficient, ω the angular frequency, and $j = \sqrt{-1}$. The real and complex components of Z_D can be separated and expressed in dimensionless variables, giving

$$Z_D = A(q) - j\,B(q) \tag{4}$$

where:

$$A(q) = \sigma\omega^{-1/2}\left[\frac{\sinh q + \sin q}{\cosh q + \cos q}\right]$$
$$B(q) = \sigma\omega^{-1/2}\left[\frac{\sinh q - \sin q}{\cosh q + \cos q}\right] \tag{5}$$

and the dimensionless variable $q = \delta(2\omega/D_o)^{1/2}$. These equations then can be used to obtain an expression for the resistive and reactive components of the impedance for the equivalent circuit in Fig. 4,

$$Z(\omega) = \frac{A'(q)\omega^{-1} - j\left(C_{DL}[A'(q)^2 + B(q)^2] + B(q)\omega^{-1}\right)}{C_{DL}^2\omega[A'(q)^2 + B(q)^2] + 2\,C_{DL}B(q) + \omega^{-1}} \tag{6}$$

where $A'(q) = A(q) + R_{ct}$. In the low-frequency limit the impedance approaches the diffusion resistance, which is given by

$$R_o = \sigma\delta\left(\frac{2}{D_o}\right)^{1/2} \tag{7}$$

The above description of the low-frequency impedance of a NiCd cell can be tested by comparing experimental impedance data with that obtained by the use of Eq. (6). In Fig. 3, the resistive and reactive components of the cell impedance are plotted as a function of $\omega^{-1/2}$ for the data of Fig. 2. These data clearly demonstrate that at least two processes influence the cell impedance, as indicated by the two peaks in the reactive component of the impedance. In general, the diffusion impedance may reflect either diffusion in the electrolyte or diffusion in surface films on either of the electrodes in the NiCd cell. Because the time constants of the two processes noted in Fig. 3 are of the same order of magnitude, we may assume they are both caused by either electrolyte or film diffusion. It is likely that each of the two processes is respectively associated with each of the electrodes in the NiCd cell. The overall cell impedance will have the form

$$Z_T(\omega) = Z_1(\omega) + Z_2(\omega) \tag{8}$$

where Z_1 and Z_2 are the impedances arising from each of the two diffusion-controlled processes and each has the form given by Eq. (6). A nonlinear fitting routine[18] (GAUSAUS) was used to simultaneously fit the resistive and reactive components of the experimentally measured impedance to Eq. (8). The fit to the data is indicated by the curves in Fig. 3. For the open circuit NiCd cell, the model represented by Eq. (8) described the cell impedance at states of charge ranging from near total discharge to about 90% of full charge. The applicability of the model was limited, because at total discharge the impedance measurement itself changes the state of charge of the cell significantly, and near full charge noise presents experimental problems.

The parameters that describe the equivalent circuit in Fig. 4 for each of the two processes are $C_T = C_s + C_{DL}$, R_{ct}, σ, and $\delta/\sqrt{D_o}$. Except at total discharge, the open circuit impedance data could be accurately modeled if we neglect R_{ct}, i.e., $R_{ct} \ll R_o$. In analyzing the data, we therefore assume

$R_{ct} \approx 0$. The charge transfer resistance is expected to be small for NiCd cells, because a large transfer resistance would prevent high-rate cell discharge.

The capacitance associated with each electrode is obtained as the sum of the double layer and surface capacitances. This capacitance was typically several hundred farads, most of which is expected to be a surface pseudo-capacitance. As indicated in Table I, the capacitance displayed wide variations for duplicate measurements. This variability implies that the electrode surfaces are difficult to precisely control over long time intervals on open circuit.

Table I. Typical NiCd Electrode Capacitances (F)

Percent State of Charge		Process 1 Capacitance	Process 2 Capacitance
88	EXP A	606	374
	B	725	305
	C	299	1099
44	EXP A	203	97
	B	492	569
	C	391	481
20	EXP A	744	321
	B	555	473
	C	751	249
0.5	EXP A	547	<1
	B	71	32
	C	67	15

As the cell neared the discharged state, the capacitance associated with the observed diffusion processes tended to decrease. For process 2 in Figs. 2 and 3, the capacitance became on the order of 10 F or less. The overall decrease in capacitance is likely to result from changes in film structure and thickness as well as from decreasing active material surface area as the cell is discharged.

Each diffusion process that can occur in a NiCd cell can be represented by a Warburg coefficient σ and a characteristic time $\delta/\sqrt{D_o}$. These parameters are plotted as a function of state of charge in Figs. 5 and 6, respectively, for the open circuit NiCd cell. Each of these data points consists of the average of three experimental determinations; the standard deviations are indicated by the error bars. The Warburg coefficient σ depends on the electrode surface area normal to the diffusion flux. The results in Fig. 5 are given in terms of geometric plate areas (which are much less than the electrochemically active surface areas), and therefore include the effects of changes in active area with state of charge. The quantitative application of the data in Figs. 5 and 6 is restricted by our limited knowledge of the surface areas involved. However, we can analyze the consistency of the data with diffusion processes involving either electrolyte transport or transport of species in a solid-state film at the active electrode surface.

If a solid film covers an electrode surface, diffusion of active species through this film must occur for charge transfer to take place. If the Warburg coefficient for diffusion is given by the equation[17]

$$\sigma = \frac{RT}{n^2F^2c\sqrt{2D_o}} \tag{9}$$

where c is the concentration in the diffusion layer, the data in Figs. 5 and 6 can be used to obtain the diffusion length δ and $c\sqrt{D_o}$ as a function of state of charge. In the case of diffusion through a solid film on the electrode surfaces, we must use σ expressed in terms of the active electrode area rather than the geometric area. The electrodes in the NiCd cell consisted of 10 positive and 11 negative sintered plates, each 6 × 7 cm. The geometric areas

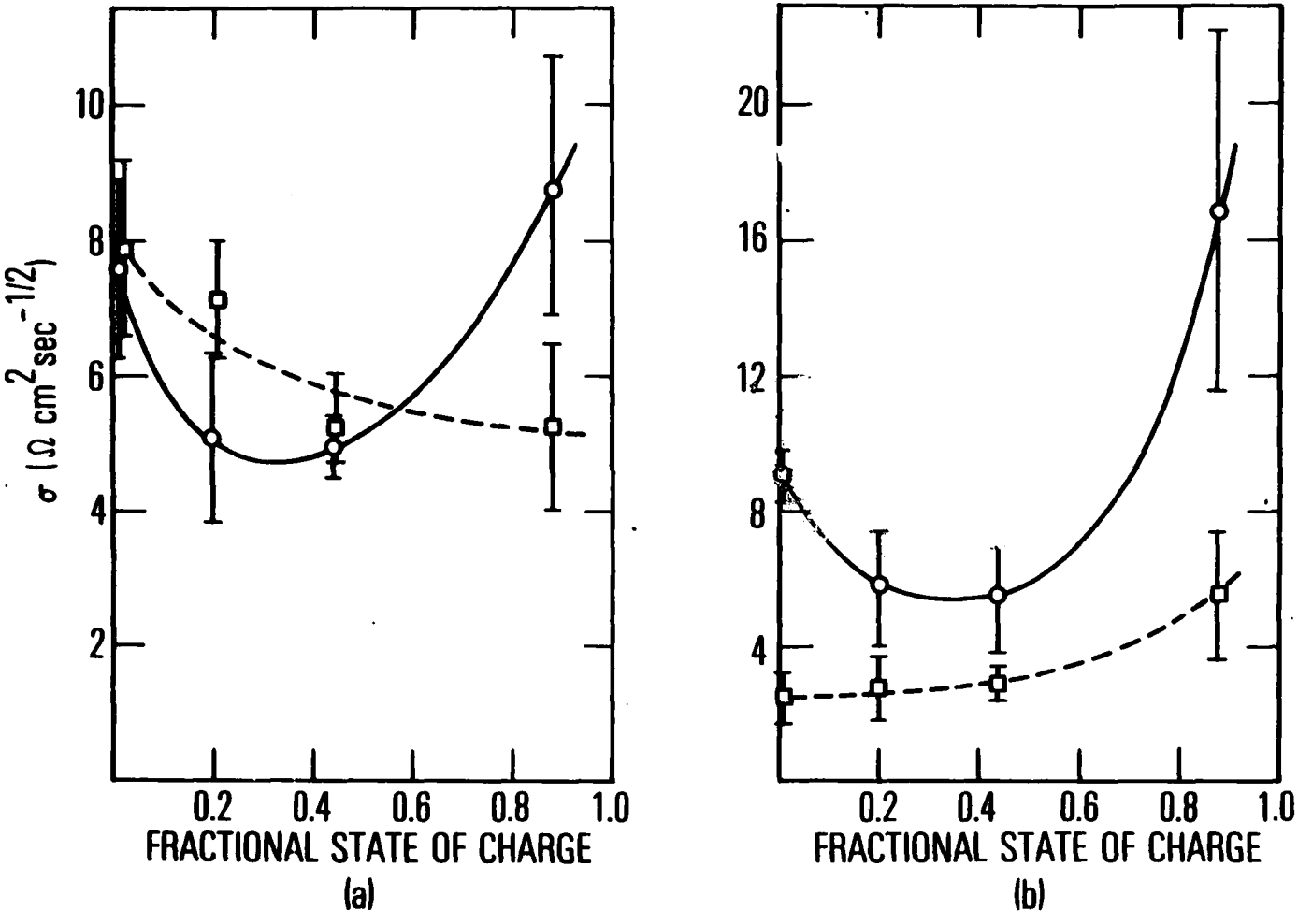

Fig. 5. Warburg Coefficient σ as a Function of State of Charge for a 10-A h Sealed NiCd Cell. The dashed lines indicate data for process 1, and the solid lines process 2. Plot (a) contains data obtained from a 1 mA charging current step, and (b) from a 1 mA discharging current step. Temperature is 25°C.

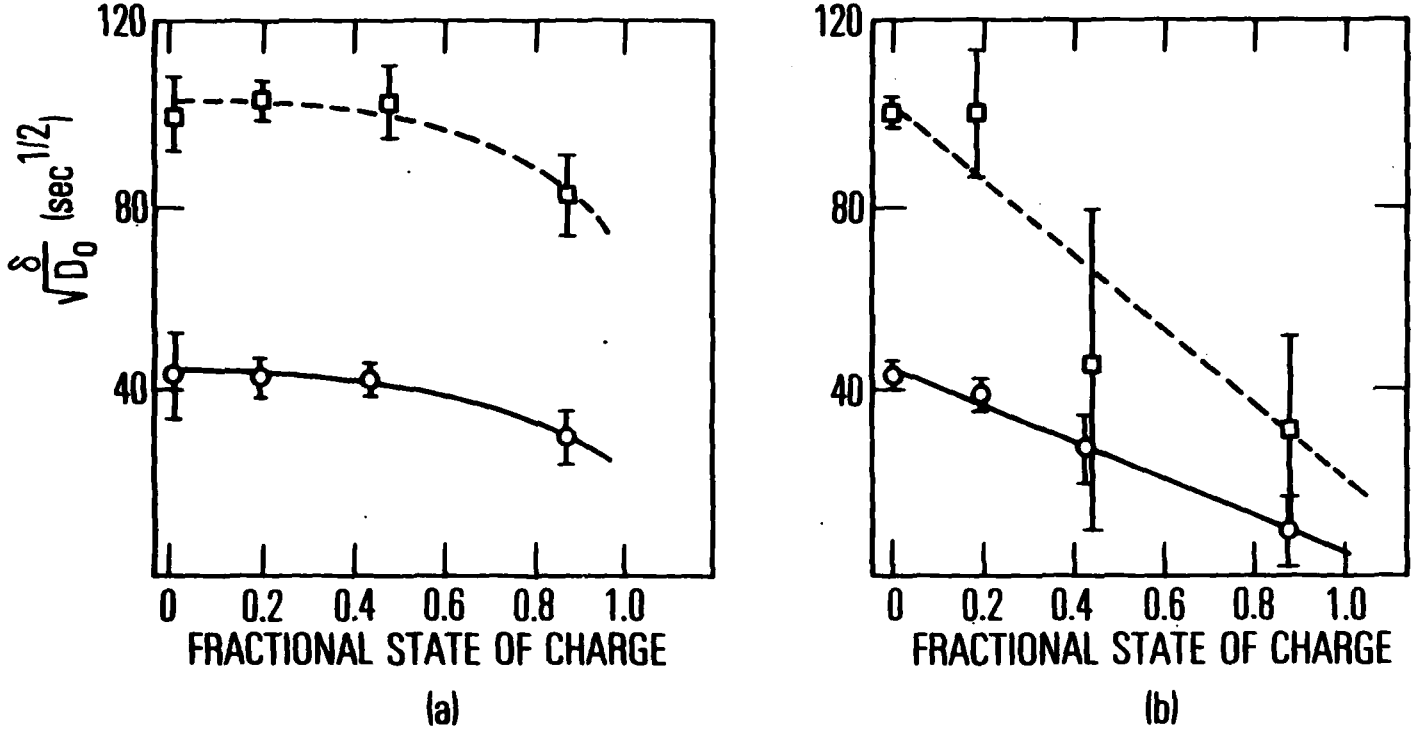

Fig. 6. Square Root of Relaxation Time for the Two Processes Observed in 10-A h Sealed NiCd Cells. The data correspond to those in Fig. 5. Temperature is 25°C.

(both sides) are 840 and 924 cm^2 for the positive and negative plates, respectively. The active surface areas, as determined from BET measurements,[19] are about 3×10^7 cm^2 and 2×10^6 cm^2 for positive and negative, respectively. The active electrochemical area must lie between these extremes, and is almost certainly more than an order of magnitude greater than the geometric area. Using 10^4 cm^2 as a lower limit for the active area and 60 Ω cm^2 $s^{-1/2}$ as a typical value for σ, $c\sqrt{D_o}$ is calculated from Eq. (9) to be less than 3×10^{-9} mole cm^{-2} $s^{-1/2}$. This limit is consistent with a film diffusion process.

Proton diffusion from the oxidation site in the NiOH lattice to the electrode-electrolyte interface is believed to be an important step in the Ni electrode reaction. Diffusion coefficients of 3.1×10^{-10} and 4.6×10^{-11} cm^2 s^{-1} have been measured by MacArthur[9] for charge and discharge, respectively, for this process. This type of proton diffusion in the solid state may result in one of the observed processes. Armstrong and Edmondson[7] have studied diffusion in solid-state films on flat Cd electrodes in the context of electrode passivation. Their work gave $c\sqrt{D_o} = 3.6 \times 10^{-10}$ mole cm^{-2} $s^{-1/2}$ and $D_o = 5 \times 10^{-10}$ cm^2 s^{-1}. Although the results are consistent with our measurements, the data of Armstrong and Edmondson were for a passivated Cd electrode, whereas in the NiCd cell we are far from passivating potentials. However, it is clear that the processes described here could arise from diffusive transport through surface films.

Since OH^- and H_2O are produced and consumed at the Ni and Cd electrodes during charge and discharge, diffusion of these electrolyte species should be considered as a possible origin for the observed processes. This kind of diffusion would involve polarization of the electrode material by the diffusion of electrolyte species through the sintered plate. The diffusion coefficient should depend on the plate structure and the morphology of the electrode surfaces, and is expected to be less than that for bulk KOH electrolyte[20] where $D_o = 2.3 \times 10^{-5}$ cm^2 s^{-1}. With the use of the geometric plate area, a typical value of σ is 6 Ω cm^2 $s^{-1/2}$, which gives $c\sqrt{D_o} = 3 \times 10^{-8}$ mole cm^{-2} $s^{-1/2}$. At 50% state of charge, the concentration of KOH electrolyte in the NiCd cell is

about 6M, which gives $D_o = 2.5 \times 10^{-11}$ cm^2 s^{-1}. If a typical value of 40 $s^{1/2}$ is used for $\delta/\sqrt{D_o}$, the diffusion length is estimated to be 2×10^{-4} cm. This is several orders of magnitude less than the plate thicknesses (7×10^{-2} cm, 30 mil). The low diffusion coefficient combined with the estimated diffusion length indicates that electrolyte diffusion may be more accurately described as a combination of limited pore diffusion in the sintered plates and diffusion of electrolyte species through the oxides with which the pores are loaded.

Electrolyte diffusion must occur for the NiCd cell to operate, and therefore this diffusion impedance is expected to be revealed somewhere in the frequency spectrum. Since only the two processes were observed, it seems likely that at least one of these is caused by electrolyte diffusion. A plausible interpretation of the data is that these two processes are associated with diffusion in the positive and negative plates, respectively. The processes are resolved in the frequency spectrum, because the pore morphology in the positive plate differs from that in the negative. The variations in σ with state of charge indicated in Fig. 5 can be qualitatively explained by Eq. (9). As the cell is discharged, the electrolyte concentration (or activity) increases, causing σ to initially drop. As discharge continues, oxide materials build up in the electrode pores, decreasing D_o and thereby causing σ to rise sharply as the discharged state is approached. The trends indicated in Fig. 6 for $\delta/\sqrt{D_o}$ may also be explained by the expected decrease in D_o as the cell is discharged.

The temperature dependence of the impedance (44% charged cell) is indicated in Fig. 7 by the dependence of σ on temperature from 10 to 40°C. The parameter $\delta/\sqrt{D_o}$ did not display a significant temperature dependence. Activation energies obtained for each diffusion process are indicated in Fig. 7. The range of about 3 kcal/mole is typical for thermal diffusion processes, and therefore the observed temperature dependence is consistent with the diffusion model employed.

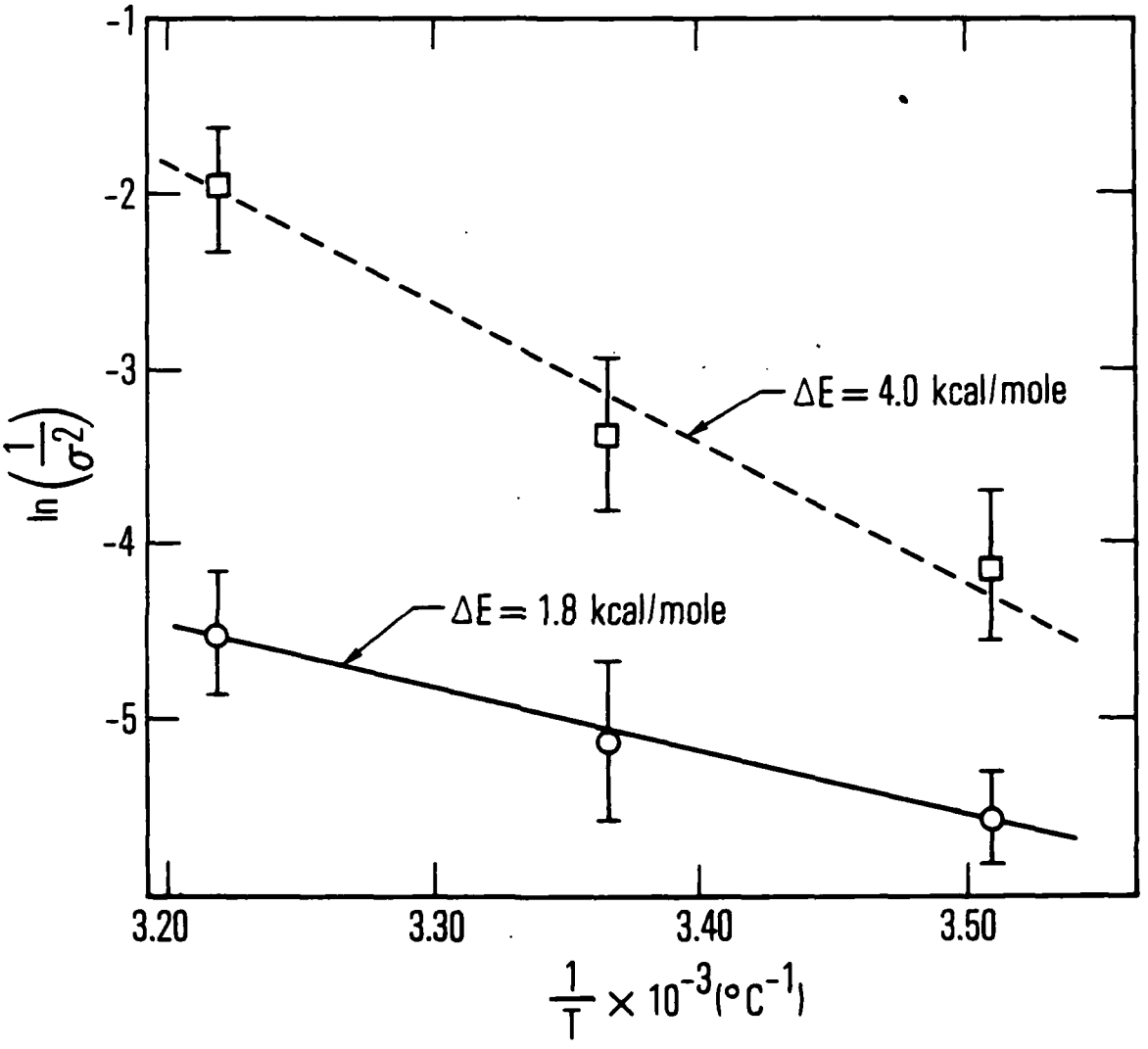

Fig. 7. Plot of Temperature Dependence of Diffusion Coefficient Assuming Concentrations Constant with Temperature. The dashed line is for process 1, and the solid line is for process 2. Activation energies represented by these lines are indicated.

V. CONCLUSIONS

The impedance of a NiCd cell has been measured over the frequency range of 0 to 10^5 Hz under open-circuit conditions. An equivalent circuit model of the cell is presented that accurately describes the low-frequency impedance in terms of two diffusion-controlled processes operating in series. Data analysis indicates that both solid-state film diffusion processes and electrolyte diffusion processes are consistent with the data. Because concentration polarization is known to occur in NiCd cells, the two observed processes are tentatively assigned to electrolyte diffusion in the positive and negative plates. These processes are resolved in the impedance spectrum because of the differences in pore structure and morphology between the positive and negative electrodes.

REFERENCES

1. R. J. Brodd and H. J. DeWane, J. Electrochem. Soc. 110, 1091 (1963).

2. M. Lurie, H. N. Seiger, and R. C. Shair, Technical Documentary Report ASD-TDR-63-191, Gulton Industries (1963).

3. P. Bauer and R. H. Sparks, Vol. I, Report No. 2315-6005-RU000, TRW Defense and Space Systems, Redondo Beach, Calif. (1 April 1963).

4. Report No. QE/C-64-6, U.S. Naval Ammunition Depot, Quality Evaluation Laboratory, Crane, Ind. (8 April 1964).

5. Report No. QE/C 65-124, U.S. Naval Ammunition Depot, Quality Evaluation Laboratory, Crane, Ind. (16 February 1965).

6. P. Bauer, Batteries for Space Power Systems, National Aeronautics and Space Administration (1968) pp. 89-95.

7. R. D. Armstrong and K. Edmondson, Electroanal. Chem. Interfacial Electrochem., 53 (1974) 371.

8. D. M. MacArthur, J. Electrochem. Soc. 117, 422 (1970).

9. D. M. MacArthur, J. Electrochem. Soc. 117, 729 (1970).

10. S. U. Falk and A. J. Salkind, Alkaline Storage Batteries, (Wiley, New York, 1969), p. 525.

11. A. H. Zimmerman and M. R. Martinelli, Transient Techniques for Low Frequency Battery Impedance Measurements, TR-0079(4970-10)-1, The Aerospace Corp., El Segundo, Calif. (6 October 1978).

12. F. Gutman, J. Electrochem. Soc. 112, 94 (1965).

13. M. Keddam, Z. Stoynov, and H. Takenouti, J. Appl. Electrochem. 7, 539 (1977).

14. J. J. Lamden and E. E. Nelson, J. Electrochem. Soc. 107, 723 (1960).

15. M. R. Martinelli and A. H. Zimmerman, Impedance Measurements on Sealed Lead-Acid Cells, ATR-78(8114)-1, The Aerospace Corp., El Segundo, Calif. (10 May 1978).

16. J. E. B. Randles, Discuss. Faraday Soc. 1, 11 (1947).

17. P. Drossbach and J. Schultz, Electrochim. Acta, 9 (1964) 1391.

18. H. J. Wertz, GAUSAUS - Nonlinear Least Squares Fitting and Function Minimization, Mathematics and Computation Center, The Aerospace Corp., El Segundo, Calif. (1968).

19. G. Halpert, Techniques of Electrochemistry, Vol. 3, E. Yeager and A. J. Salkind, ed., (Wiley, New York, 1978), pp. 336 - 342.

20. Falk and Salkind, Op. Cit., p. 591.

LABORATORY OPERATIONS

The Laboratory Operations of The Aerospace Corporation is conducting experimental and theoretical investigations necessary for the evaluation and application of scientific advances to new military space systems. Versatility and flexibility have been developed to a high degree by the laboratory personnel in dealing with the many problems encountered in the nation's rapidly developing space systems. Expertise in the latest scientific developments is vital to the accomplishment of tasks related to these problems. The laboratories that contribute to this research are:

Aerophysics Laboratory: Launch vehicle and reentry aerodynamics and heat transfer, propulsion chemistry and fluid mechanics, structural mechanics, flight dynamics; high-temperature thermomechanics, gas kinetics and radiation; research in environmental chemistry and contamination; cw and pulsed chemical laser development including chemical kinetics, spectroscopy, optical resonators and beam pointing, atmospheric propagation, laser effects and countermeasures.

Chemistry and Physics Laboratory: Atmospheric chemical reactions, atmospheric optics, light scattering, state-specific chemical reactions and radiation transport in rocket plumes, applied laser spectroscopy, laser chemistry, battery electrochemistry, space vacuum and radiation effects on materials, lubrication and surface phenomena, thermionic emission, photosensitive materials and detectors, atomic frequency standards, and bioenvironmental research and monitoring.

Electronics Research Laboratory: Microelectronics, GaAs low-noise and power devices, semiconductor lasers, electromagnetic and optical propagation phenomena, quantum electronics, laser communications, lidar, and electro-optics; communication sciences, applied electronics, semiconductor crystal and device physics, radiometric imaging; millimeter-wave and microwave technology.

Information Sciences Research Office: Program verification, program translation, performance-sensitive system design, distributed architectures for spaceborne computers, fault-tolerant computer systems, artificial intelligence, and microelectronics applications.

Materials Sciences Laboratory: Development of new materials: metal matrix composites, polymers, and new forms of carbon; component failure analysis and reliability; fracture mechanics and stress corrosion; evaluation of materials in space environment; materials performance in space transportation systems; analysis of systems vulnerability and survivability in enemy-induced environments.

Space Sciences Laboratory: Atmospheric and ionospheric physics, radiation from the atmosphere, density and composition of the upper atmosphere, aurorae and airglow; magnetospheric physics, cosmic rays, generation and propagation of plasma waves in the magnetosphere; solar physics, infrared astronomy; the effects of nuclear explosions, magnetic storms, and solar activity on the earth's atmosphere, ionosphere, and magnetosphere; the effects of optical, electromagnetic, and particulate radiations in space on space systems.


DAT
FILM